Plant Physiology and Biochemistry 229 (2025) 110502

Contents lists available at ScienceDirect

Plant Physiology and Biochemistry

journal homepage: www.elsevier.com/locate/plaphy

Insights into metabolic profile and redox adjustment during ammonium-induced salt acclimation in sorghum plants

Stelamaris de Oliveira Paula-Marinho [a,e,*], Rafael de Souza Miranda [b,e], Gyedre dos Santos Araújo [a], Isabelle Mary Costa Pereira [a,e], Rosilene Oliveira Mesquita [c,e], Sergimar Kennedy de Paiva Pinheiro [d], Emílio de Castro Miguel [d], Lineker de Sousa Lopes [a], Humberto Henrique de Carvalho [a,e], Enéas Gomes-Filho [a,e,**]

[a] Department of Biochemistry and Molecular Biology, Federal University of Ceará, Fortaleza, Brazil
[b] Department of Plant Science, Federal University of Piauí, Teresina, Brazil
[c] Department of Plant Science, Federal University of Ceará, Fortaleza, Brazil
[d] Department of Metallurgical and Materials Engineering, and Analytical Center, Federal University of Ceará, Fortaleza, Brazil
[e] National Institute of Science and Technology in Salinity (INCTAgris / CNPq), Federal University of Ceará, Fortaleza, Brazil

ARTICLE INFO

Keywords:
Nitrogen nutrition
Chloroplast ultrastructure
Metabolic profile
Oxidative stress

ABSTRACT

The role of external nitrogen source (NO_3^- or NH_4^+) against salinity-promoted damage on photosynthetic machinery and primary metabolism was investigated in *Sorghum bicolor* L. Sorghum growth was severely decreased by salinity, but the damage was less pronounced in NH_4^+-fed plants. Closely, NH_4^+ nutrition promoted better CO_2 uptake rate, associated with higher phosphoenolpyruvate carboxylase activity and maintenance of photosystem II efficiency, as well as better ionic regulation in comparison to NO_3^- nutrition. In parallel, although NH_4^+ nutrition induced high basal H_2O_2 content, minor damage to chloroplast integrity was observed compared to NO_3^- after saline stress. In non-saline conditions, NH_4^+-fed plants exhibited more connected network than NO_3^- nutrition, which led to decreased salt impact in network parameters after salt stress. This may be related to previous changes during acclimatization to NH_4^+, allowing quick responses to secondary stresses, such as salinity. A metabolite set was significantly modulated by N source under salinity, including amino acids, sugar, and organic acids metabolism that displayed important contribution in response to salt stress. The asparagine amino acid was considered a key metabolite in alleviating NH_4^+ toxicity. Despite the unchanged antioxidant enzymes system, NH_4^+ nutrition increased the content of ascorbic acid, which may contribute to redox homeostasis and protect the chloroplasts against oxidative damage under salinity. Therefore, NH_4^+ nutrition was able to activate mechanisms involved in photosynthetic efficiency and regulation of important metabolites, which attenuated the deleterious effects of salinity on sorghum plants.

1. Introduction

Nitrogen (N) is an essential element in plant metabolism. It is a structural component of diverse molecules, such as chlorophyll, amino acids, proteins and nucleic acids. In soil solution, N is available as nitrate (NO_3^-) and ammonium (NH_4^+) that are absorbed by channels and transporters in roots and assimilated into amino acids in plastids (Zayed et al., 2023). Nitrogen nutrition has shown to be an assertive strategy to mitigate deleterious effects of abiotic stress in plants, such as salinity, where the degree of stress tolerance is associated with N form in the growth medium in a species-dependent manner (Tavakoli et al., 2025). Most plant species prefer NO_3^- or mixed-N (NO_3^-:NH_4^+) nutrition because only NH_4^+ nutrition can disturb plant growth and metabolism (Boschiero et al., 2019; de Souza et al., 2021). However, other species have presented tolerance and elevated performance under NH_4^+ nutrition, and NH_4^+ source may fulfill a positive role in the cross-tolerance to abiotic stress (Miranda et al., 2017; Li, 2024).

Salt stress is widely cited as a severe abiotic stress that disrupts both

This article is part of a special issue entitled: Plant stress responses published in Plant Physiology and Biochemistry.

* Corresponding author. Department of Biochemistry and Molecular Biology, Federal University of Ceará, Fortaleza, Brazil.
** Corresponding author. Department of Biochemistry and Molecular Biology, Federal University of Ceará, Fortaleza, Brazil.
E-mail addresses: maris.biologa@gmail.com (S.O. Paula-Marinho), egomesf@ufc.br (E. Gomes-Filho).

https://doi.org/10.1016/j.plaphy.2025.110502
Received 30 June 2025; Received in revised form 30 August 2025; Accepted 8 September 2025
Available online 9 September 2025

osmotic and ionic homeostasis, promoting over accumulation of toxic ions and oxidative damage in the tissues that impair plant metabolism and growth (Zhou et al., 2024). The salinity-induced oxidative stress is characterized by excessive production and accumulation of reactive oxygen species (ROS). The ROS may damage nucleic acids, proteins and membrane lipids, impairment enzymes functioning, well as cause degradation or decreased synthesis of photosynthetic pigments, disrupt the chloroplast integrity, reduction of photochemical efficiency, and finally activate programmed cell death (Allel et al., 2018; Manaa et al., 2019).

The plant responses to salinity are complex by including different scales. The phenotypic differences result from interaction of elements with stress, such as transcriptomic, proteomic and metabolomic changes (Jia et al., 2019; Oliveira et al., 2020). Metabolomic studies may provide a holistic understanding to comprehend and preview the pathway regulation and alterations related to tolerance or susceptibility to salt stress. The metabolic approach has revealed key metabolites that can be used to characterize genotypes and identify distinct levels of salt tolerance, as observed among *Oryza sativa* cultivars (Chang et al., 2019). It reported the salt impact on pathways involving energy metabolism, sugar metabolism, biosynthesis of phytohormones and amino acids profile (Jia et al., 2019; Rajkumari et al., 2023). The plotting of N-mediated metabolite reprogramming may provide insight of plant molecular and physiological responses to alleviate salt stress. However, evidence into how N nutrition, specifically N source, modulates the metabolic profile of salt stressed sorghum plants remains unclear.

Plants develop diverse strategies to cope with the effects of salinity. These include a Na^+ exclusion, accumulation of osmolytes for osmotic adjustment, and enhancement of the antioxidant system (Hualpa-Ramirez et al., 2024). Previous studies reported that NH_4^+ nutrition may constitute an efficient strategy to activate ionic- and oxidative-related metabolic pathways and counteract salinity damage, as observed to *Citrus sinensis* and *Zea mays* (Hessini et al., 2019; Fernández-Crespo et al., 2014). It suggests that NH_4^+ nutrition may led to an "acclimation stage", contributing to better responses to salt stress.

Sorghum bicolor has been recognized as a salt-tolerant crop (Lacerda et al., 2005) that exhibits remarkable physiological and biochemical adjustments under exclusive NH_4^+ nutrition. The NH_4^+-mediated salt tolerance have been attributed to (i) accumulation of amino acids for osmotic adjustment, contributing to water status maintenance, osmoprotection and decreased salinity-induced K^+ efflux (Miranda et al., 2013, 2016; Coelho et al., 2020); (ii) synthesis of proteins associated with energy metabolism (Oliveira et al., 2020), enabling the redirection of energy toward proton pump activity in roots, ultimately supporting the regulation of SOS1 and NHX antiporters (Miranda et al., 2017); (iii) the restriction of Na^+ uptake by root, which reduces Na^+ loading into the xylem sap and its subsequent accumulation in shoots (Miranda et al., 2017; Coelho et al., 2020); and (iv) the de novo synthesis or upregulation of proteins related to the photosynthetic apparatus (Oliveira et al., 2020). Nevertheless, the beneficial effects of nitrogen nutrition in antioxidative defense, protection of photosynthetic apparatus, and metabolic adjustment of salt-stressed sorghum remain unclear.

Our working hypothesis was that NH_4^+ nutrition improves antioxidative and metabolic traits that promote protection of photosynthetic apparatus and salt tolerance in sorghum plants. The hypothesis was tested by assessing growth, photosynthesis, chloroplast integrity, photochemical efficiency, ROS production and scavenging in leaves of sorghum exposed to salinity under different N sources.

2. Materials and methods

2.1. Plant material and growth condition

Forage sorghum seeds [*Sorghum bicolor* (L.) Moench] cv. CSF 20 were provided by Instituto Agronômico de Pernambuco (IPA, Pernambuco, Brazil). They were sown in vermiculite moistened with distilled water, and after four days uniform seedlings were transferred to nutrient solution at 1/3 ionic strength. Hoagland's nutrient solution was modified to contain 5.0 mM nitrogen, supplied with the isolated forms of NO_3^- and NH_4^+ (Table S1), and renewed every three days. Salt treatments were imposed 12 days after sowing, by adding 75 mM NaCl (Miranda et al., 2013, 2016), and samples were harvested after 12 days of stress imposition. During the experiments, environmental conditions were as follows: midday photosynthetic photon flux density, approximately 1,200 μmol m^{-2} s^{-1}, mean temperature of 32.2 ± 2 °C during the day, 25.9 ± 1 °C at night, and mean relative humidity of 63.4 ± 16 %.

2.2. Growth and photosynthetic parameters

Leaf area (LA) was measured using a leaf area meter (LI-3100C, Li-Cor®). The plant material was divided into shoot and roots, and dried in air circulation oven at 60 °C for 72h to provide the shoot and root dry mass (SDM and RDM, respectively).

Gas exchange and chlorophyll *a* fluorescence were measured in last fully expanded leaves from the base before harvest, using a portable photosynthesis system (IRGA, model Li-6400XT, Li-Cor®) with an artificial light source [photosynthetic photon flux density (PPFD = 1,200 μmol photon m^{-2} s^{-1})] and coupled to a fluorometer (model 6400-40, Li-Cor®). The CO_2 concentration in the chambers was approximately 380 μmol mol^{-1}. Values of CO_2 assimilation rate (*A*), stomatal conductance (g_s) and intercellular CO_2 concentration (*Ci*) were estimated from 9:00 to 11:00h a.m. These values were used to calculate the *Ci/Ca* ratio (*Ca* as ambient CO_2 concentration) and instantaneous carboxylation efficiency (*A/Ci*). Chlorophyll *a* fluorescence parameters were measured after 30 min adaptation to the dark, being assessed Fm (dark maximum fluorescence), Fo (dark minimum fluorescence), Fm' (light maximum fluorescence), Fs (light steady-state fluorescence) and Fo' (light minimum fluorescence after the far-red illumination). Then, the values were used to estimated effective quantum yield of PSII (ΦPSII), maximum quantum yield of PSII (Fv/Fm), photochemical [qP = (Fm' - Fs)/(Fm' - Fo')] and non-photochemical [NPQ = (Fm - Fm')/Fm'] quenching, and electron transport rate [ETR = ΦPSII × PPFD × 0.5 × 0.84].

2.3. Phosphoenolpyruvate carboxylase activity

The enzyme extract was prepared from fresh leaves, using solution containing 100 mM Tris-HCl buffer (pH 7.5), 5.0 % glycerol, 10 mM $MgCl_2$, 1.0 mM ethylenediaminetetraacetic acid (EDTA), 1.0 mM sodium orthovanadate (Na_3VO_4), 5.0 mM dithiothreitol (DTT), 2.0 % polyvinylpyrrolidone (PVP), and 1 mM phenylmethanesulfonyl fluoride (PMSF). Phosphoenolpyruvate carboxylase activity was measured by NADH oxidation kinetics in the presence of malate dehydrogenase (MDH) enzyme, using the NADH molar extinction coefficient (6.22 mM^{-1} cm^{-1}) at 340 nm, according to Echevarria et al. (1994). The reaction medium was composed by 100 mM HEPES-KOH buffer (pH 8.0), 5.0 mM $MgCl_2$, 2.5 mM phosphoenolpyruvate (PEP), 1.0 mM $NaHCO_3$, 0.2 mM NADH, and 5.0U mL^{-1} MDH enzyme at 30 °C. Protein concentration in the crude extracts was determined according to Bradford (1976), using bovine serum albumin (Sigma-Aldrich, USA) as standard.

2.4. Inorganic ions contents

Samples from dried leaf or root were incubated in deionized water at 45 °C for 1h, and then centrifuged at 3000×*g* for 15min. The supernatants were collected and used as crude extracts to determine the contents of K^+ and Na^+. Na^+ and K^+ contents were measured by flame photometry (model B462, Micronal®), according to Malavolta et al. (1989).

2.5. Ultrastructure of chloroplasts

Leaf sections (1–2 mm^2) were fixed using 5.0 % glutaraldehyde in 50 mM phosphate buffer (pH 7.2) and post-fixed in 2.0 % (w/v) OsO_4 in the

same buffer (Omoto et al., 2013). After dehydrated in a graded acetone series, the sections were embedded in epoxy resin (Embed 812). Ultra-sections (70 nm) were obtained using an ultramicrotome (model UC7, Leica®), stained with uranyl acetate and lead citrate double contrast, and examined in a transmission electron microscope (JEM 1011, JEOL®) at an accelerating voltage of 100 kV.

2.6. ROS production in leaves by confocal laser scanning microscopy

Detection of ROS in freehand sections of sorghum leaves was performed as described by Freitas et al. (2018) with minor modifications. The sections were incubated on a solution of 2′,7′-dichlorofluorescein diacetate (DCFH-DA) (Sigma Aldrich®) at 50 μM on 10 mM phosphate buffer (pH 7.0) for 30min at dark. After washing with the same buffer, the sections were immediately observed under Ar laser (λ = 488 nm), using confocal laser scanning microscope (CLSM) (LM 710, Zeiss®). Excitation signals were collected between 500 and 580 nm. The control images were performed only under HeNe laser (λ = 633 nm) related to chlorophyll *b* autofluorescence, producing emission signals between 638 and 721 nm. Digital images were acquired using 20x magnification objective lens and serial images were reconstructed with Carl Zeiss LSM software. The fluorescence intensity for emission of DCFH-DA was measured in twenty sections of three images captured using Zen® software.

2.7. Contents of $\bullet O_2^-$, H_2O_2 and lipid peroxidation

Crude extracts were prepared by homogenizing 0.5g of fresh mass from leaves in 50 mM phosphate buffer (pH 7.8) and in 100 mM potassium phosphate buffer solution (pH 6.3), for superoxide radical ($\bullet O_2^-$) and hydrogen peroxide (H_2O_2) extraction, respectively. Spectrophotometric readings at 530 nm were carried out in supernatant to measure $\bullet O_2^-$ content using $NaNO_2$ solution as standard curve (Elstner and Heupel, 1976). Whereas H_2O_2 concentration was determined following reaction medium containing 12 mM phenol, 0.5 mM 4-aminoantipyrine, 84 mM phosphate buffer (pH 7.0), 1.0U mL^{-1} horseradish peroxidase (HRP) and plant extract (Fernando and Soysa, 2015). The absorbance was measured at 505 nm and compared with a standard curve obtained from increasing H_2O_2 concentrations.

Lipid peroxidation was assayed by monitoring the malondialdehyde (MDA) absorbance (Heath and Packer, 1968). Fresh leaves were briefly ground in 5 % trichloroacetic acid (TCA), at 4 °C. After centrifuged at 10, 000×*g* for 15min, an aliquot of the supernatant was mixed with solution of 0.5 % thiobarbituric acid (TBA) in 20 % TCA and heated at 95 °C in water bath for 30min. MDA content was calculated through the difference between the absorbance at 532 and 600 nm, using the molar extinction coefficient of 155 mM^{-1} cm^{-1}.

2.8. Antioxidant enzymes

For antioxidant enzyme activities, samples of fresh leaves were homogenized in 100 mM phosphate buffer (pH 7.0) with 0.1 mM ethylenediaminetetraacetic acid (EDTA) at 4 °C. After centrifugation at 12,000×*g*, at 4 °C, the supernatant was collected and used to measure the enzyme activity. Protein concentration in the crude extracts was estimated by absorbance at 595 nm, according to Bradford (1976), using bovine serum albumin as standard.

Enzyme activities were assayed in a 96-well microplate reader (Synergy HTX, BioTek®), performing kinetic activity during 10min at 30 °C, except for superoxide dismutase (SOD; EC 1.15.1.1). Ascorbate peroxidase (APX; EC 1.11.1.11) activity was measured as described by Nakano and Asada (1981), using the molar extinction coefficient for ascorbate (2.8 mM^{-1} cm^{-1}). Catalase (CAT; EC 1.11.1.6) activity was determined by consumption of H_2O_2 monitored at 240 nm as described for Beers and Sizer (1952), employing the molar extinction coefficient (36 M^{-1} cm^{-1}). Guaiacol peroxidase (GPOD; EC 1.11.1.7) activity was measured according to Urbanek et al. (1991), using the molar extinction coefficient for tetraguaiacol (26.6 mM^{-1} cm^{-1}). APX, CAT and GPOD activities were expressed as μmol H_2O_2 min^{-1} mg^{-1} protein.

The SOD activity was determined according to Beyer and Fridovich (1987) by absorbance reading of blue formazan at 560 nm, produced by photoreduction of the nitroblue tetrazolium (NBT), after 15min under light (two 20-W fluorescent tubes) at 25 °C. SOD activity was determined as the amount of enzyme required to cause 50 % inhibition of the NBT photoreduction, it was expressed as enzyme unit (EU mg^{-1} of protein).

2.9. Primary metabolites extraction and analysis

The extracts of polar metabolites were obtained as described by Lisec et al. (2006) with minor modifications, with solution containing methanol, chloroform and ultrapure water (2:1:2, v/v). Aliquot of upper water-methanol (polar) phase was transferred to a new tube and dried in a vacuum concentrator at room temperature. For derivatization step, the dried samples were treated with methoxylamine hydrochloride (20 mg mL^{-1}) in anhydrous pyridine with shake at 37 °C for 2h, followed by the addition of N-methyl-N-(trimethylsilyl)-trifluoro acetamide (MSTFA) with shake at 37 °C for 30min.

The primary metabolites were obtained using gas chromatography coupled to mass spectrometry (GC-MS, QP-PLUS, model 2010; Shimadzu, Japan). One microliter sample was injected in split mode (1:5 ratio). Helium was used as carrier gas with a flow rate of 1.2 mL min^{-1}. The RTX-5MS capillary column (30m × 0.25 mm × 0.25 μm) was used to separate metabolites, being programed with an initial temperature at 80 °C for 2min, then ramped of 10 °C per min to 315 °C, and held for 8min. The injection and ion source temperature were kept at 250 °C and the MS interface temperature was set at 230 °C. The mass spectrometer operated at 70eV (EI) and used scan range of 40–700 (m/z), initiated after solvent cut time of 3min. Quality control (QC) samples were injected alternated with biological samples (every 7–8 samples) to monitor the instrument quality, well as blanks were injected to solvent control for each batch processing. All chromatographic peaks were individually integrated in every sample to ensure they fit a normal distribution and have an appropriate baseline.

Both chromatogram and mass spectra analysis were evaluated using XcaliburTM 2.1 software, being compared with public Golm Metabolome Database library and with an internal library constructed by mixture of standard of some sugars and amino acids. The data were normalized to the internal standard (ribitol), in each chromatogram, and the sample fresh mass, being expressed as the relative area concentration. After the normalization of the data, chemometric analysis was performed by MetaboAnalyst 6.0 (https://www.metaboanalyst.ca/), as well as one-it was generated a heatmap comparing the abundance of metabolites among the treatments.

2.10. Metabolic network analysis

Metabolic network was built based on the correlation analysis of all metabolites and the nitrogen source under salt stress. The size of a node reflects the importance of metabolites, and its degree of connectivity in each network of nitrogen source, and the links are the strength of debiased sparse partial correlation (DSPC) coefficient (*r*) (Basu et al., 2017). The blue link represents negative correlation coefficient, while red link indicates positive correlation among the nodes of network. The networks were created by using the Metscape on Cytoscape® software, using restricting *r* values between $-0.8 < r > 0.8$ to select the most important metabolites. The density, heterogeneity and centralization of networks were obtained using NetworkAnalyzer on Cytoscape® software.

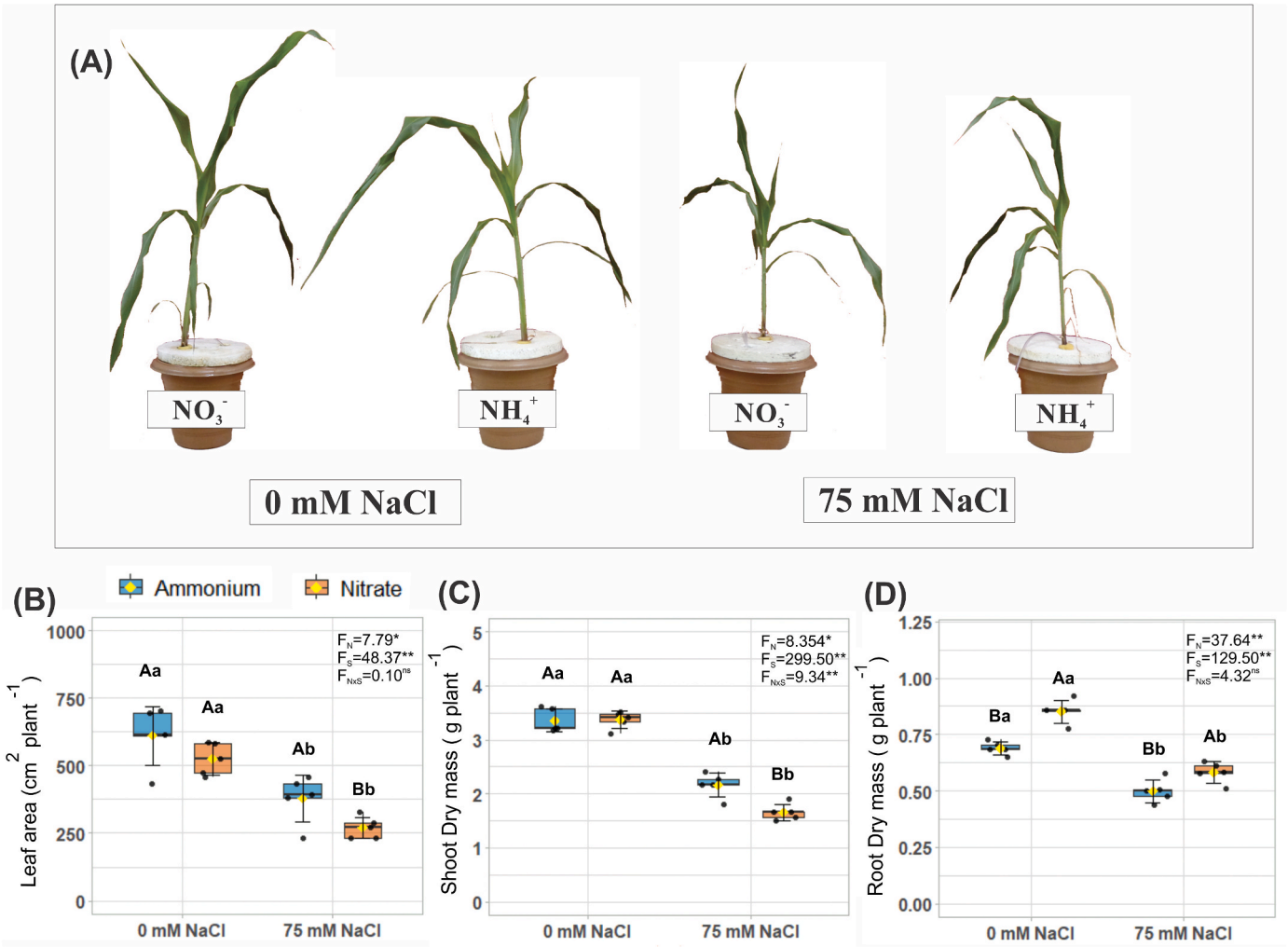

Fig. 1. Phenotypic appearance of representative plants (**A**), leaf area (**B**), and shoot (**C**) and root (**D**) dry masses of *Sorghum bicolor*, cv. CSF 20, grown with different nitrogen nutrition (NO_3^- or NH_4^+) and exposed to absence (0 mM NaCl) or presence of 75 mM NaCl for 12 days. Boxplot representing the means (yellow point) ± standard deviations (SD) of n = 5 (black points). In the same NaCl level, different capital letters indicate significant differences due to nitrogen nutrition, whereas different lowercase letters denote significant differences due to NaCl concentration in the same nutrition, according to Tukey's test ($p < 0.05$). F values from ANOVA: *significant at 5 %; **significant at 1 %; ^{ns} nonsignificant to nitrogen source (N), salinity (S) and interaction (NxS). (For interpretation of the references to color in this figure legend, the reader is referred to the Web version of this article.)

2.11. Experimental design and statistical analysis

The experimental design was completely randomized in a 2 × 2 factorial scheme, composed of two nitrogen sources (NO_3^- and NH_4^+) and two salt levels [0 and 75 mM NaCl], with five biological replicates, except to metabolomic analysis that used four replicates. Data were subjected to a two-way analysis of variance (ANOVA), and the mean values were compared by Tukey's test ($p < 0.05$), using Sisvar 5.6 program.

The files with relative concentration of metabolites for leaves tissues of sorghum under each treatment were normalized by log transformation and auto scaling to improve the data quality for statistical analysis by MetaboAnalyst 6.0 server (http://www.metaboanalyst.ca). Principal Component Analysis (PCA) was performed to identify the differences in metabolic composition among the N source (NO_3^- and NH_4^+) in absence (0 mM NaCl) and presence of salt stress (75 mM NaCl), as well as the data was submitted to a one-way ANOVA to identify the significant metabolites.

3. Results

3.1. Plant growth parameters and modulation of photosynthetic machinery

Salinity promoted a significant decrease in *S. bicolor* growth as compared to plants grown in non-saline condition (0 mM NaCl) (Fig. 1A). Under saline condition, NH_4^+-fed stressed plants showed higher shoot dry mass and LA than NO_3^--fed stressed plants, while the root dry mass exhibited opposite trend (Fig. 1B, C and D). There are no changes in LA and shoot dry mass of plants under ammonium or nitrate in the absence of salt, although ammonium nutrition reduced root dry mass.

In general, the net photosynthetic rate (*A*) was higher in plants grown with NH_4^+ nutrition in both salinity levels (0 and 75 mM NaCl) (Fig. 2A), while nonsignificant difference occurred in stomatal conductance (g_s) (data no showed, $F_N = 0.18^{ns}$, $F_S = 1.01^{ns}$, $F_{NxS} = 0.12^{ns}$). On this hand, a reduced intercellular CO_2 concentration (*Ci*) was found in plants grown with NH_4^+ source, resulting in lower *Ci/Ca* ratio compared to NO_3^--plants (Fig. 2B and C). Salt stress increased the *Ci* in plants grown with NO_3^-, while no significant difference occurred in NH_4^+-fed plants. Also, NH_4^+-supplied plants showed higher values of Rubisco

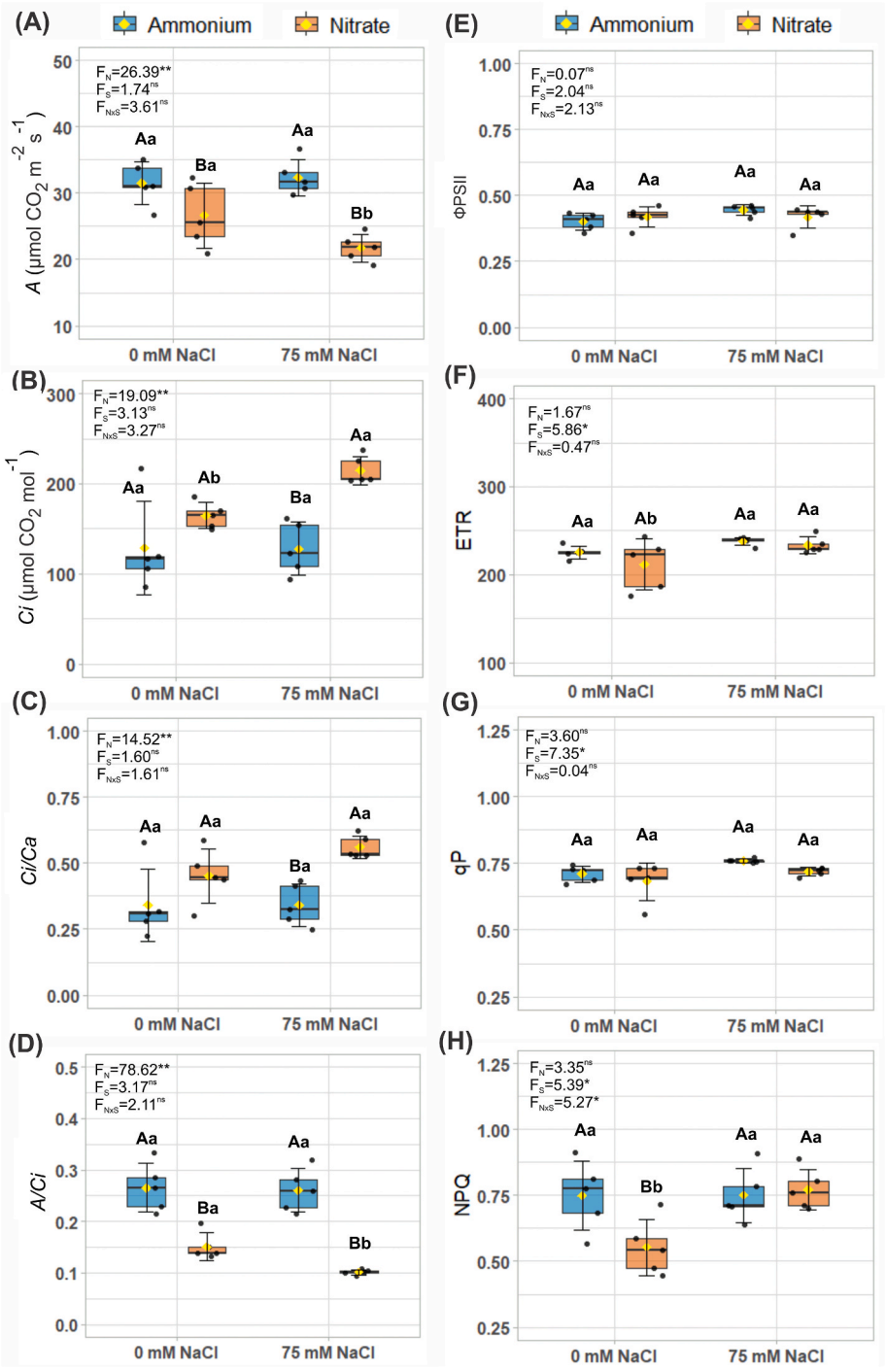

Fig. 2. Gas exchange parameters [CO_2 assimilation rate (**A**), intercellular CO_2 concentration (**B**), *Ci/Ca* ratio (**C**) and instantaneous carboxylation efficiency of Rubisco - *A/Ci* (**D**)] and chlorophyll *a* fluorescence parameters [effective quantum yield of PSII – ΦPSII (**E**), electron transport rate – ETR (**F**), photochemical quenching – qP (**G**), and non-photochemical quenching – NPQ (**H**)] of sorghum plants, cv. CSF 20, grown in the absence (0 mM NaCl) or presence of 75 mM NaCl under different nitrogen nutrition (NO_3^- or NH_4^+) for 12 days. Boxplot representing the means (yellow point) ± standard deviations (SD) of n = 5 (black points). Statistical details are the same as in Fig. 1. (For interpretation of the references to color in this figure legend, the reader is referred to the Web version of this article.)

carboxylation efficiency (*A/Ci*) than NO_3^--fed plants, in both NaCl levels (Fig. 2D). Regarding chlorophyll *a* fluorescence parameters, nonsignificant difference was observed in the effective quantum yield of PSII (ΦPSII) and photochemical quenching (qP) under saline condition. However, salt stress significantly increased the non-photochemical quenching (NPQ) and ETR in plants grown with NO_3^- source when compared to control plants in NaCl absence (Fig. 2F and H). On the other hand, NH_4^+-fed plants exhibited no changes in NPQ and ETR values in relation to non-stressed plants.

3.2. Phosphoenolpyruvate carboxylase activity

The phosphoenolpyruvate carboxylase activity was affected only by interaction of the factors (N source and salinity level). NO_3^--grown stressed plants showed significant decrease in enzyme activity compared to non-stressed plants, with activity values lower than those of NH_4^+-fed

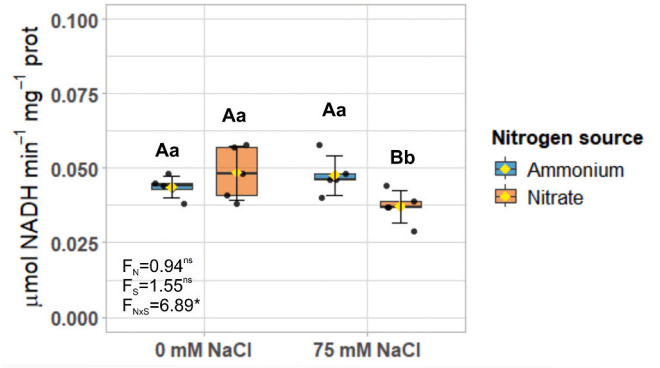

Fig. 3. Phosphoenolpyruvate carboxylase activity in leaves of *Sorghum bicolor*, cv. CSF 20, grown with different nitrogen nutrition (NO_3^- or NH_4^+) and exposed to absence (0 mM NaCl) or presence of 75 mM NaCl for 12 days. Boxplot representing the means (yellow point) ± standard deviations (SD) of n = 5 (black points). Statistical details are the same as in Fig. 1. (For interpretation of the references to color in this figure legend, the reader is referred to the Web version of this article.)

plants (Fig. 3).

3.3. Ion homeostasis in leaves and roots

Salt stress condition dramatically decreased K^+ content in leaves and roots of sorghum plants in both nitrogen nutrition (NO_3^- and NH_4^+ source). However, NH_4^+-fed plants presented higher K^+ contents in both tissues under salinity, compared to NO_3^- (Fig. 4A and C). An opposite trend was exhibited for Na^+ accumulation, in which salinity increased the Na^+ content, but the lowest Na^+ contents under salinity were found in leaves and roots of NH_4^+-fed plants (Fig. 4B and D). The treatments did not show significant differences in the K^+/Na^+ ratio in leaves and roots.

3.4. Ultrastructure of chloroplasts and oxidative stress in sorghum leaves

The ultrastructure of chloroplasts from mesophyll cells of sorghum plants was investigated by transmission electron microscopy from three replicates (Fig. 5, Fig. S1). The electro micrographs revealed well-developed granum in all nitrogen treatments, as well as a few plastoglobuli in the absence of salinity (Fig. 5A and B). Moreover, there was a significant change in the ultrastructure of thylakoids and an increase in the number of plastoglobuli under 75 mM NaCl stress. Salt stress provoked the swelling in grana, resulting in wavy thylakoids in NO_3^--plants (Fig. 5C), with no apparent wavy thylakoids in NH_4^+-fed plants (Fig. 5D). The morphology of bundle sheath chloroplasts was also investigated, but there was no clear alteration due to salt stress or nitrogen nutrition (data not shown).

Through confocal laser scanning microscope, the probe 2′,7′-dichlorofluorescein diacetate (DCFH-DA) was employed to monitor the ROS production, mainly H_2O_2 (green color), in leaf cells of sorghum plants subjected to different treatments (Fig. 6A–E). Under absence of salinity, H_2O_2 fluorescence was detected mainly in mesophyll cells of sorghum plants from all nitrogen nutrition (Fig. 6A and B), with a high but no significant fluorescence emission found in NH_4^+-fed plants (Fig. 6F). Even though NH_4^+ nutrition promoted H_2O_2 synthesis soon, after salt stress exposure, an over emission of green fluorescence was detected in leaves of plants in both mesophyll and bundle sheath cells, especially in NO_3^--fed stressed plants as compared the NO_3^--fed unstressed plants (Fig. 6D and F).

The salt-induced oxidative stress also was detected by ROS accumulation in leaves of sorghum. In general, salinity promoted a higher superoxide radical ($\bullet O_2^-$) and H_2O_2 content in plants grown with NO_3^- as sole N source than in plants at 0 mM NaCl (Fig. 6G and H). Likewise,

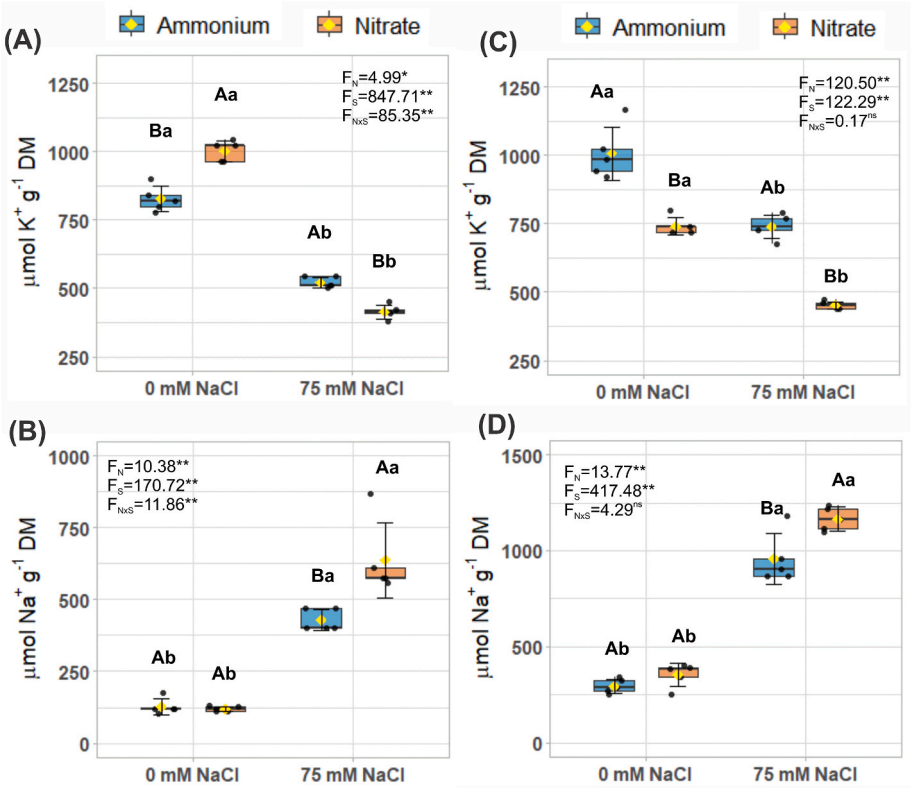

Fig. 4. K^+ and Na^+ of leaves (**A**, **B**) and roots (**C**, **D**), respectively, of *Sorghum bicolor*, cv. CSF 20, grown with different nitrogen nutrition (NO_3^- or NH_4^+) and exposed to absence (0 mM NaCl) or presence of 75 mM NaCl for 12 days. Boxplot representing the means (yellow point) ± standard deviations (SD) of n = 5 (black points). Statistical details are the same as in Fig. 1. (For interpretation of the references to color in this figure legend, the reader is referred to the Web version of this article.)

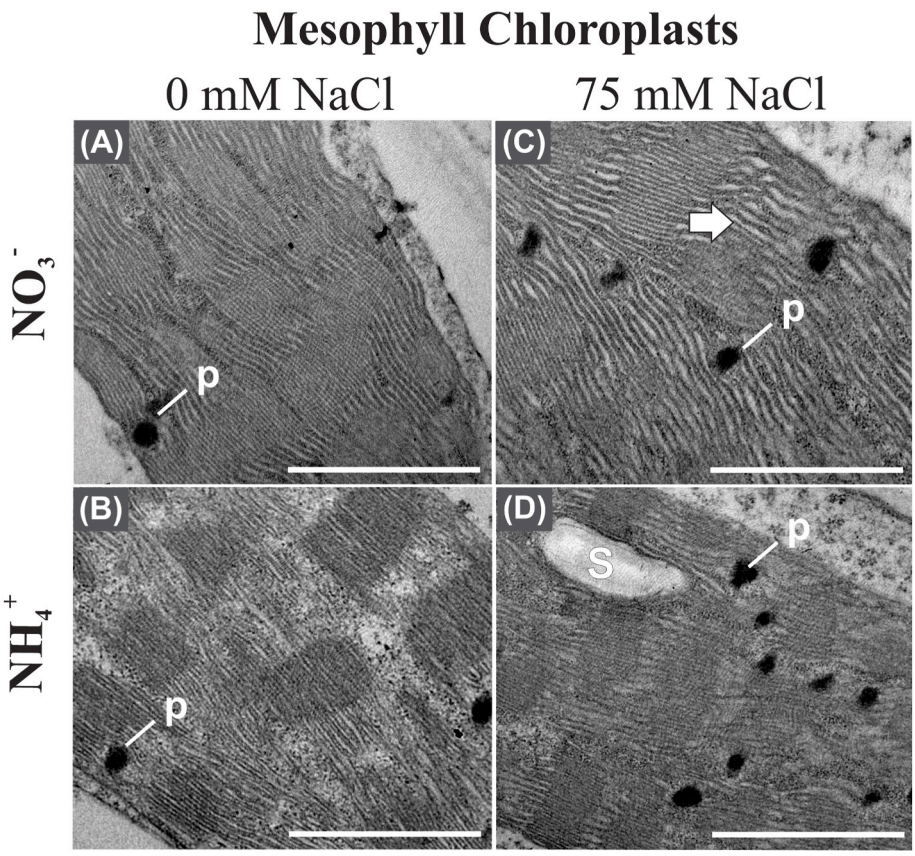

Fig. 5. Representative transmission electron micrographs of chloroplasts from mesophyll of *Sorghum bicolor*, cv. CSF 20, grown with nitrogen nutrition (NO_3^- or NH_4^+) and exposed to absence (0 mM NaCl) or presence of 75 mM NaCl for 12 days. (**A**) NO_3^- + 0 mM NaCl; (**B**) NH_4^+ + 0 mM NaCl; (**C**) NO_3^-+ 75 mM NaCl and (**D**) NH_4^+ + 75 mM NaCl. White arrows – Wavy thylakoids, p – Plastoglobuli, S – Starch grain. Bar = 1 μm.

membrane lipid peroxidation (estimated by MDA content) was drastically increased by salt stress only in leaves from NO_3^--plants compared to absence of NaCl (Fig. 6I). Interestingly, NH_4^+-fed plants showed no significant alteration by salt stress in leaf H_2O_2 and $\bullet O_2^-$ contents, as well as MDA level (Fig. 6G, H and I).

3.5. Antioxidant enzymatic system activity

In NaCl absence, NH_4^+-fed plants displayed elevated ascorbate peroxidase (APX) activity, and decreased catalase (CAT) and guaiacol peroxidase (GPOD) activities in relation to plants grown with nitrate as N source (Fig. 7A, B and C). Conversely, APX activity decreased in leaves of stressed plants grown with NH_4^+ (Fig. 7A), while NO_3^--fed plants exhibited significant decline in CAT activity under salt stress compared to non-stressed plants (Fig. 7C). Besides, SOD was not affected by salinity neither by N source (Fig. 7D).

3.6. Primary metabolism responses from leaves of sorghum

Primary metabolites analysis identified a total of 67 metabolites from leaves of sorghum grown with different nitrogen sources (NO_3^- and NH_4^+) under salinity and non-salinity condition, including amino acids, sugar and derivates (sugar phosphate and sugar alcohol), amines, organic acids, phenolic compounds and vitamins (Table S2). Sugar and derivates (26) were the majority of identified metabolites, followed by organic acids (19) and amino acids (16).

PCA analysis of metabolic profile indicated a clear separation of the N sources in both NaCl conditions, through the PC1 explaining 49.2 % of variance and PC2 with 16.6 % for the difference among metabolic profiles of sorghum leaves in response to N source and salinity levels (Fig. 8A). The loading plots of each PCA showed the contribution of detected metabolites for separating the groups (Fig. 8B–Table S3). Herein, the most dominating metabolites in PC1 were lactic acid (1), succinic acid (2), malic acid (3), fumaric acid (4) and malonic acid (5) (Fig. 8B).

To assess the metabolic dynamic of N nutrition and salinity, the abundance of the 52 significant metabolites was plotted in a heatmap, showing the clusters formed between the N sources (Fig. 9). Under salt stress, NH_4^+ nutrition promoted a higher accumulation of some amino acids, like asparagine, aspartic acid, threonine, lysine, phenylalanine, and others, compared to stressed plants grown with NO_3^- (Fig. 9). By contrast, NO_3^--fed plants exhibited mainly higher abundance in organic acids in comparison to other N nutrition, lactic acid, pantothenic acid, pyruvic acid, for example, as well as those belonging to the tricarboxylic acid (TCA) cycle, such as succinic acid, malic acid, 2-oxoglutaric acid. The ascorbic acid accumulation was higher in NH_4^+-fed plants in both saline levels, while putrescine content was pooler accumulated in NO_3^--fed plants. The post-hoc comparisons from statistical results are shown in Table S4, with the significant differences and *p* value, according to Tukey's test.

3.7. Metabolomics network

Correlation-based metabolic networks explored the relationship among significant metabolites in response to different nitrogen nutrition in the absence and presence of salinity (Fig. 10). The number of links, density, heterogeneity, and hubs number of each drawn network are shown in Table S5. All the networks were arranged in an only array with the 52 significant metabolites of ANOVA test. In non-salinity conditions, NH_4^+ network showed higher hubs and links numbers in relation to NO_3^- network, while an opposite pattern was observed under salt stress (Fig. 10A and C; Table S5). Under salt stress, network of NH_4^+ nutrition

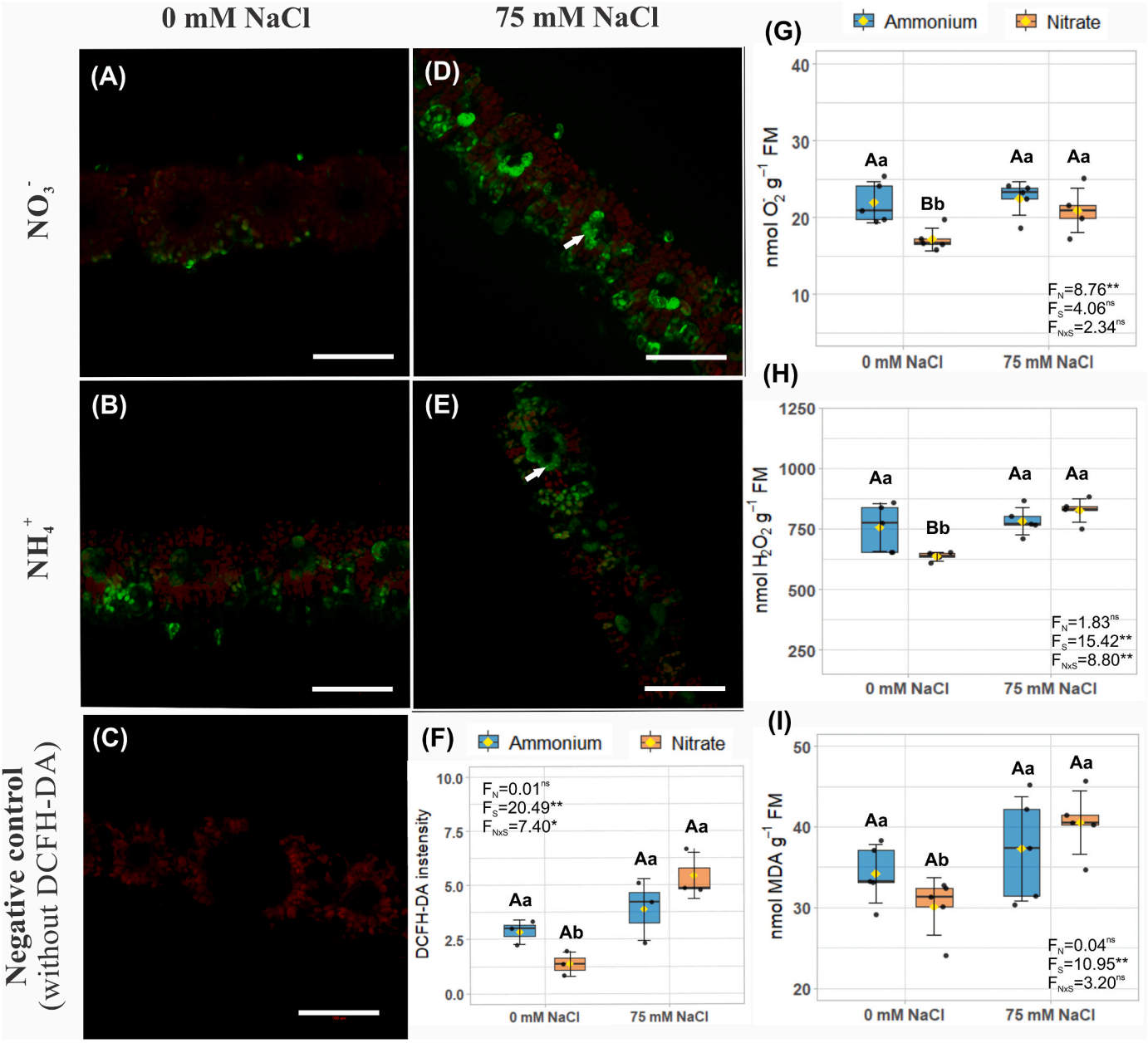

Fig. 6. ROS detection [*in vivo* – green fluorescence; 2′,7′-dichlorofluorescein diacetate (DCFH-DA) probe] in leaves of *Sorghum bicolor*, cv. CSF 20, grown with nitrogen nutrition (NO_3^- or NH_4^+) and exposed to absence (0 mM NaCl) or presence of 75 mM NaCl for 12 days. (**A**) NO_3^- + 0 mM NaCl; (**B**) NH_4^+ + 0 mM NaCl; (**C**) negative control; (**D**) NO_3^- + 75 mM NaCl and (**E**) NH_4^+ + 75 mM NaCl. White arrow = H_2O_2 production in bundle sheath cell, and red color = chlorophyll *b* autofluorescence. Bar = 100 μm. Fluorescence intensity for emission of DCFH-DA (**F**); superoxide radical ($\bullet O_2^-$, **G**), hydrogen peroxide (H_2O_2, **H**) and malondialdehyde (MDA, **I**) contents in leaves of sorghum plants. Boxplot representing the means (yellow point) ± standard deviations (SD) of n = 5 (black points). Statistical details are the same as in Fig. 1. (For interpretation of the references to color in this figure legend, the reader is referred to the Web version of this article.)

exhibited density and heterogeneity values of 0.181 and 0.256, respectively, which were lower than those in non-saline conditions (0.202 and 0.339, respectively) (Table S5). On the other hand, under NO_3^- nutrition, salt stress increased density and heterogeneity compared to network of non-stressed plants.

It was considered hubs the metabolites that exhibited number of links higher than the mean of the network links. In sorghum grown with NO_3^-, the network of non-stressed plants showed 25 hubs, increasing to 33 hubs in salt stressed plants (Fig. 10A). Under salt stress, the network of NO_3^--fed plants presented new hubs as dehydroascorbic acid, glutamine, trehalose and asparagine (Fig. 10B). Yet, under NH_4^+ nutrition, the network at 0 mM NaCl showed 26 hubs, like pyruvic acid, citric acid, asparagine and sucrose (Fig. 10C; Table S5). However, after salinity imposition, the metabolic network of the NH_4^+-grown plants presented a reduction of hubs number (to 23 hubs) compared to those of non-stressed treatment, but with 13 new hubs like as valine, fructose, phenylalanine and ascorbic acid (Fig. 10D; Table S5).

4. Discussion

Salinity is a serious environmental factor that negatively influences the growth, yield and physiological mechanisms of several plant species (Zhou et al., 2024). Alterations in N sources by replacing total or partially NO_3^- for NH_4^+ have emerged as a promisor strategy to alleviate salinity damage in numerous plant species, highlighting activation of defense mechanisms to withstand deleterious salt effects (Miranda et al.,

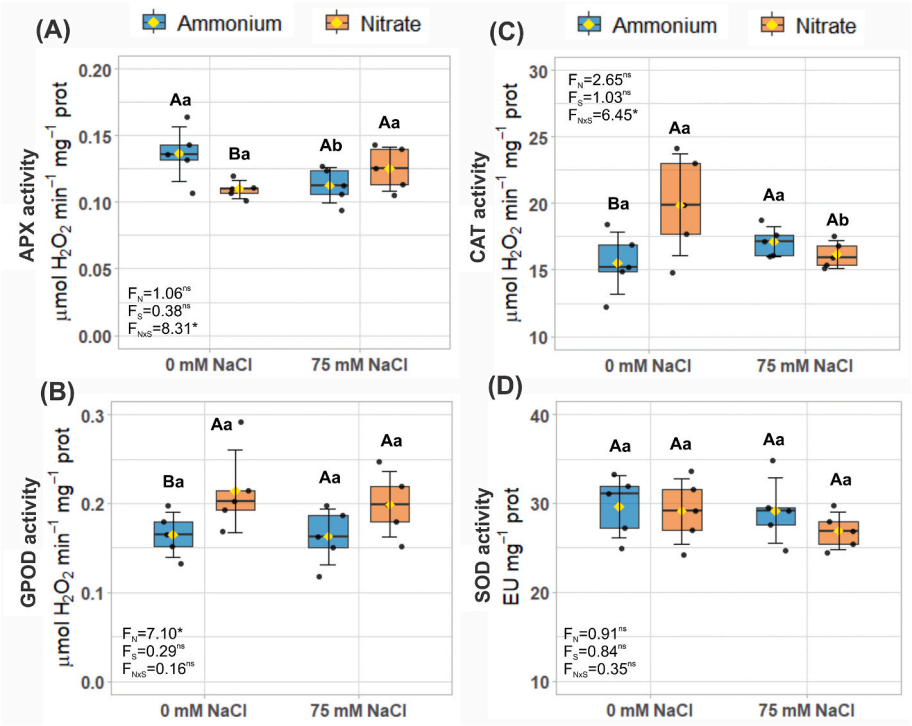

Fig. 7. Activity of ascorbate peroxidase - APX (**A**), guaiacol peroxidase - GPOD (**B**), catalase - CAT (**C**) and superoxide dismutase - SOD (**D**) in leaves of *Sorghum bicolor*, cv. CSF 20, grown with different nitrogen nutrition (NO_3^- or NH_4^+) and exposed to absence (0 mM NaCl) or presence of 75 mM NaCl for 12 days. Boxplot representing the means (yellow point) ± standard deviations (SD) of n = 5 (black points). Statistical details are the same as in Fig. 1. (For interpretation of the references to color in this figure legend, the reader is referred to the Web version of this article.)

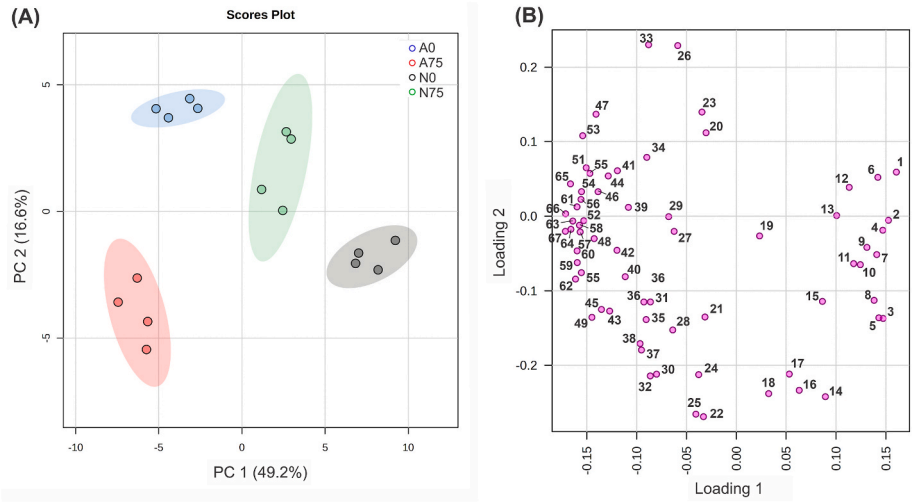

Fig. 8. Principal component analysis - PCA (**A**) and loading plot of metabolites (**B**) of *Sorghum bicolor* leaves, cv. CSF 20, grown with different nitrogen nutrition (NO_3^- or NH_4^+) and exposed to absence (0 mM NaCl) or presence of 75 mM NaCl for 12 days. [(N0) NO_3^- + 0 mM NaCl; (N75) NO_3^- + 75 mM NaCl; (A0) NH_4^+ + 0 mM NaCl, and (A75) NH_4^+ + 75 mM NaCl]. The metabolite enumeration is listed in Supplementary Table S3.

2017; Hessini et al., 2019; Oliveira et al., 2020; de Souza et al., 2021). Herein, we provide evidence into how ammonium nutrition counteracts salt damage in ultrastructure and functioning of photosynthetic machinery, ionic homeostasis and primary metabolism for salt tolerance of *S. bicolor* plants.

4.1. *Ammonium-induced salt tolerance is associated with favorable ionic homeostasis and CO_2 assimilation*

The ability to keep the ion homeostasis is crucial for salinity resilience in plants, a response closely associated with a capacity to mitigate the salt-induced toxicity effects in cells (Miranda et al., 2017; Oliveira et al., 2020; Zhou et al., 2024). Higher cellular Na^+ content causes membrane depolarization impacting the uptake of other nutrients due to competition by sites and transporters and channels, especially K^+ (Kronzucker et al., 2013). The reduced sorghum growth under 75 mM NaCl-stress seemed to be related to ionic balance disruption, mainly by Na^+ increase in tissues (Figs. 1, 4B and D). Clearly, our findings evidence that NH_4^+ nutrition promoted a favorable ionic regulation and better shoot growth compared to NO_3^- source, a response

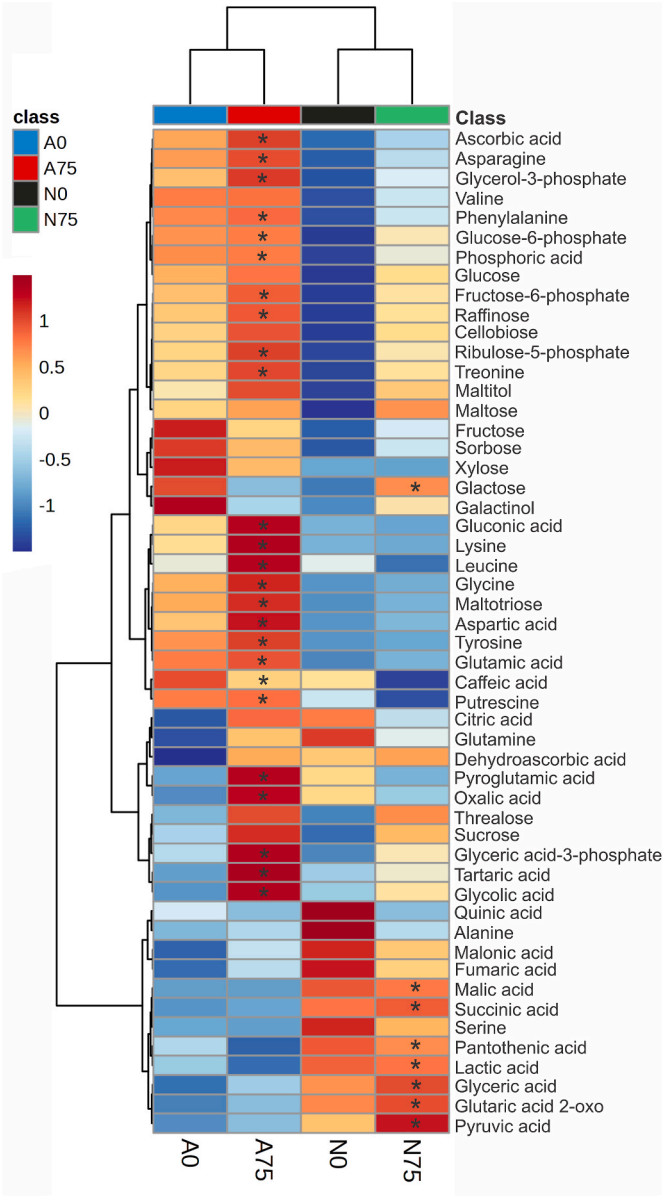

Fig. 9. Heat map representation of the relative abundance of 52 most significant metabolites in leaves of *Sorghum bicolor* leaves, cv. CSF 20, grown with different nitrogen nutrition (NO_3^- or NH_4^+) and exposed to absence (0 mM NaCl) or presence of 75 mM NaCl for 12 days of treatments. [(N0) NO_3^- + 0 mM NaCl; (N75) NO_3^- + 75 mM NaCl; (A0) NH_4^+ + 0 mM NaCl, and (A75) NH_4^+ + 75 mM NaCl]. Metabolites with asterisks indicate significant difference between N source under salinity (75 mM NaCl).

associated with lower Na^+ accumulation and favorable K^+ levels in leaves (Figs. 1B, 4A and B). The adjustment of NH_4^+-induced ionic homeostasis result from increased Na^+ extrusion by fine-tuning of SOS transporters and proton pumps in sorghum roots, as well as increased K^+ uptake by high-affinity transporters (Alvarez-Pizarro et al., 2011; Miranda et al., 2017; Coelho et al., 2020).

The leaf K^+/Na^+ homeostasis was crucial for photosynthetic performance under salt stress, since Na^+ overaccumulation may lead to ROS accumulation and inhibit the CO_2 assimilation enzymes (Manaa et al., 2019; Oliveira et al., 2020), particularly phosphoenolpyruvate carboxylase (PEPCase) and Rubisco (Liang et al., 2023). Salinity decreased the PEPCase activity in NO_3^--fed plants compared to non-stressed plants, a response associated with the reduction of gas exchange (Figs. 2A and 3). Nevertheless, NH_4^+-supplied plants showed PEPCase activity and gas exchange parameters similar to non-saline plants. It may be related to the NH_4^+-induced signal response mediated by secondary messenger, such as nitric oxide (NO), involving post-translational regulation of proteins and putrescine contents (Baena et al., 2017; Zhu et al., 2018). Hence, NH_4^+ nutrition mitigated salt deleterious effects on photosynthesis, promoting better performance of sorghum plants under salinity.

4.2. *Ammonium promotes priming phenomenon to protect photosynthetic machinery under salt stress*

Salt-induced impairment of the biochemical phase of photosynthesis is currently associated with disruptions in chloroplast ultrastructure, decreased levels of photosynthetic pigments and metabolites, and compromised enzymatic activities, all closely linked to oxidative stress (Wungrampha et al., 2018; Liang et al., 2023). To investigate the impact of N nutrition in photosynthetic machinery efficiency of salt-stressed sorghum plants, the chlorophyll *a* fluorescence, ultrastructure of chloroplasts and ROS production were examined (Figs. 2E-H, 5 and 6).

The restrictions in photosynthetic efficiency of NO_3^--fed plants seemed not due to photochemical limitations originated from photoinhibition, once ΦPSII and qP were unaltered by salinity. Instead, the increase in NPQ was possibly activated to improve thermal dissipation is an attempt to avoid photodamage in PSII and protecting, at least in part, the photosynthetic apparatus from excess energy under salinity, a response demonstrated in plants under stressful conditions (Guidi et al., 2019). Additionally, the NO_3^--fed plants also failed to activate antioxidant system for ROS scavenging (showed unchanged enzymes activity) (Fig. 7), as well exhibited significant decreasing in CAT activity under salinity in comparison to plants grown with NH_4^+ source, resulting in elevated sensibility to NaCl-stress (Singh et al., 2019). The low antioxidant defense under NO_3^- nutrition resulted in swelling of chloroplasts (Omoto et al., 2013), associated with increasing ROS accumulation and MDA content (Araújo et al., 2021), an indicative of lower physiological performance under salt stress (Figs. 1, 5 and 6).

Differently, NH_4^+ nutrition was beneficial for sorghum plants under salinity, allowing elevated photosynthetic performance and growth under stressful conditions (Figs. 1 and 2A). Surprisingly, under control conditions, NH_4^+ as solely nitrogen source promoted an accumulation of H_2O_2 (Fig. 6), resulting in a slightly damaged membrane (Fig. 6I), without a drastic alteration in thylakoids membranes after salt stress (Fig. 5B). These findings suggest that NH_4^+ promotes H_2O_2 generation fine-tuning for signaling events, which, in turn, acts as a second messenger activating downstream targets to cope with harmful effects of salt (Mittler, 2017; Huang et al., 2019). Accordingly, NH_4^+-fed sorghum plants neither present ROS overproduction nor suffer oxidative damage under salinity (Fig. 6B–E, F and I), preserving the integrity of thylakoids (Fig. 5D) and photosynthetic performance (Fig. 2). This ammonium-induced protection of photosynthetic machinery and performance is not closely related to changes in enzymatic antioxidant system.

4.3. *Metabolic adjustment reveals new insights into amino acids and antioxidants for NH_4^+-mediated salt tolerance*

The N sources promoted interactive effects on amino acids, organic acids, sugars and other metabolites, corroborating with distinguished metabolic profiles under salt stress (Figs. 8 and 9). Alterations in metabolic pathways contribute to plant acclimation, the metabolic networks generated provide insights into holistic adjustments plants in response to stress, ensuring sustained development and growth (Sweetlove and Fernie, 2005). Our results showed that metabolism dynamic after salt stress was differential to each N source, considering only the 52 significant metabolites by Tukey's test (Fig. 10). Plants grown with NH_4^+ decreased the hubs number, connection degree and heterogeneity of metabolic network after salt stress (Table S5), whereas an

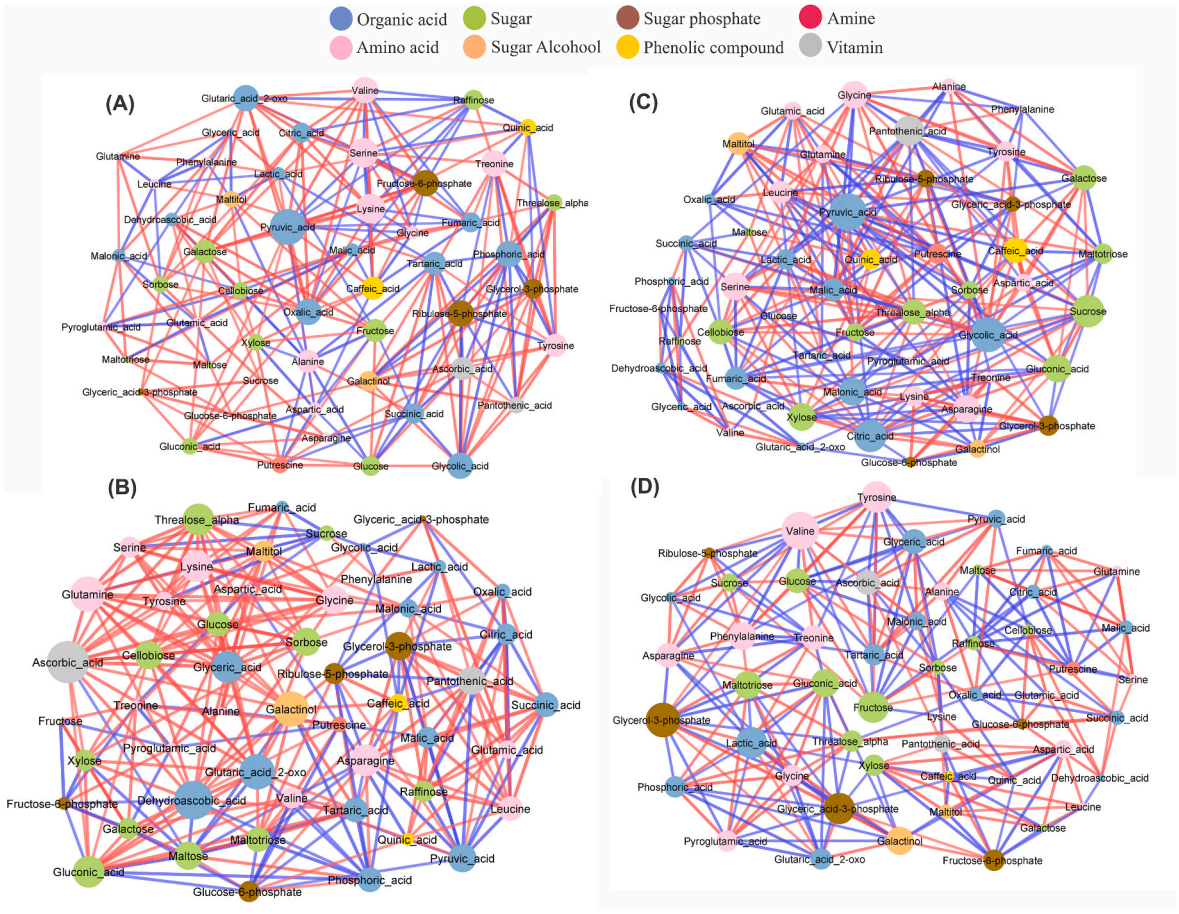

Fig. 10. Correlation-based networks of significant metabolites from leaves of *Sorghum bicolor* plants grown with different N source, NO_3^- (**A**, **B**) or NH_4^+ (**C**, **D**), and submitted for twelve days under absence (0 mM NaCl – **A**, **B**) and presence of salt stress (75 mM NaCl – **B**, **C**). The nodes are the significant metabolites (Tukey's test $p < 0.05$) and selected through of the restricting *r* values between $-0.8 < r > 0.8$. Red and blue links represent positive and negative correlation, respectively, among the nodes, whereas the thickness and the intensity of the links indicate the strength of the correlations among the metabolites. Bigger nodes denote a higher degree of connection. (For interpretation of the references to color in this figure legend, the reader is referred to the Web version of this article.)

opposite pattern in metabolic network was observed to NO_3^--fed plants (Fig. 10). The higher connectivity of NO_3^--network can represent adjustment of metabolism to respond to stress condition (Souza and Lüttge, 2015). We suggest that NO_3^--fed plants required an elevated energy cost to acclimation salinity, that was reflected by higher abundance of organic acids including tricarboxylic acid (TCA) cycle intermediates, such as succinic acid and malic acid (Munns et al., 2020). Conversely, in non-saline conditions, the NH_4^+ nutrition in itself provided higher metabolic adjustment, resulting in more connected network than NO_3^- nutrition. It seems to contribute to the diminishing of salt impact in the network parameters. Nevertheless, it is worth emphasizing, the stress response pattern varies depending on the species, as well as the type and intensity of stress (Cardoso et al., 2023).

The amino acids content is closely regulated by external N source, being reported a high enhancement in plants under NH_4^+ nutrition (Miranda et al., 2016). In accordance, NH_4^+-fed sorghum plants displayed increased amino acids accumulation, highlighting asparagine, which was evidenced as hub in metabolic networks under both control and salt conditions (Figs. 9 and 10C and D). The higher asparagine content in NH_4^+ nutrition may play a role in the reduction of NH_4^+ toxic effects in leaves, as well as controlling the C/N status (González-Hernández et al., 2019; Coelho et al., 2020). In addition, the higher sugar and sugar phosphate accumulation, as well as TCA cycle intermediates upregulated (citric acid, oxalic acid) induced by NH_4^+ nutrition may be involved in carbon flux to energy demand, synthesis of osmoprotectants and maintaining of physiological functions (Panda et al., 2021; Zi et al., 2024), acting together in acclimation on cellular processes in sorghum exposed to stress.

Specific amino acids may act as compatible solutes for osmotic adjustment to maintain water uptake and cellular turgor under salinity (Zi et al., 2024). Here, plants fed with NH_4^+ accumulated more glycine than NO_3^--fed ones, regardless of salt exposure. It is considered an important metabolite in NH_4^+ plants, and ranked as a major hub in the metabolic network (Fig. 10C and D). Amino acids like proline and glycine are frequently accumulated into the cells, contributing with tolerance response to salinity (Marco et al., 2019). Putrescine content was also accumulated in plants grown with NH_4^+ nutrition (Fig. 8), that can be related to arginine metabolism. These modulations are crucial for antioxidative defense and protein homeostasis under stress conditions (Seo et al., 2019).

The metabolites ascorbic acid and dehydroascorbic acid are currently related to redox potential in plants, which act as antioxidant defense in response to salinity (Taïbi et al., 2016). The ascorbic acid also acts in the growth and developmental process, promoting crosstalk among redox-regulated pathway and hormones (Ortiz-Espín et al., 2018). In our study, this metabolite was identified as hub in the metabolic network after salt stress imposition and classified as potential biomarker to salinity. Thus, the elevated ascorbic basal level under NH_4^+ nutrition may contribute to counteracting salt damage in chloroplast integrity (Fig. 5D) and promoted better photosynthetic activity (Figs. 1 and 2) (Ivanov, 2014; Ahanger et al., 2020).

5. Conclusion

Our investigative study highlights the beneficial role of NH_4^+ nutrition in mitigating the salt harmful effects in sorghum plants. The enhanced NH_4^+ nutrition-induced photosynthetic performance was attributed to (i.) reduced accumulation of toxic ions in leave tissues, (ii.) suppression of salt-induced ROS production and lipid peroxidation, and (iii.) maintenance of photochemical efficiency and chloroplast integrity. Otherwise, antioxidant enzymatic system seems not to be a determinant factor in salt tolerance. Different N sources promote distinct adjustments in primary metabolism, with specific patterns in the metabolic network. NH_4^+-fed plants modulate the amino acids metabolism, mainly asparagine, as a way to avoid toxic levels of NH_4^+, which result in synthesis of compounds to act as antioxidants pool (ascorbic acid) to confer increased salt tolerance in sorghum plants. The findings offer detailed insights into the physiological and metabolic adjustments of sorghum to N sources under salt stress. These data can inform future research and breeding strategies aimed at developing salt-tolerant sorghum varieties.

CRediT authorship contribution statement

Stelamaris de Oliveira Paula-Marinho: Writing – review & editing, Writing – original draft, Visualization, Validation, Supervision, Resources, Project administration, Methodology, Investigation, Formal analysis, Data curation, Conceptualization. **Rafael de Souza Miranda:** Writing – review & editing, Writing – original draft, Validation, Supervision, Data curation, Conceptualization. **Gyedre dos Santos Araújo:** Writing – review & editing, Methodology, Formal analysis, Data curation. **Isabelle Mary Costa Pereira:** Writing – review & editing, Methodology, Formal analysis, Data curation. **Rosilene Oliveira Mesquita:** Writing – review & editing, Methodology, Formal analysis, Data curation. **Sergimar Kennedy de Paiva Pinheiro:** Writing – review & editing, Methodology, Formal analysis. **Emílio de Castro Miguel:** Writing – review & editing, Methodology, Formal analysis. **Lineker de Sousa Lopes:** Writing – review & editing, Methodology. **Humberto Henrique de Carvalho:** Writing – review & editing, Writing – original draft, Supervision, Methodology, Formal analysis. **Enéas Gomes-Filho:** Writing – review & editing, Writing – original draft, Visualization, Methodology, Formal analysis, Conceptualization.

Declaration of competing interest

The authors declare that they have no known competing financial interests or personal relationships that could have appeared to influence the work reported in this paper.

Acknowledgments

This work was supported by the Conselho Nacional de Desenvolvimento Científico e Tecnológico (CNPq), National Institute of Science and Technology in Salinity (INCTAgris / CNPq), the Coordenação de Aperfeiçoamento de Pessoal de Nível Superior (CAPES) for schorlarships. We also thank Central Analítica-UFC/CT-INFRA/MCTI-SISANO/Pró-Equipamentos CAPES and Instituto Agronômico de Pernambuco (IPA) for technical support and seeds donation, respectively.

Appendix A. Supplementary data

Supplementary data to this article can be found online at https://doi.org/10.1016/j.plaphy.2025.110502.

Data availability

Data will be made available on request.

References

Ahanger, M.A., Aziz, U., Alsahli, A.A., Alyemeni, M.N., Ahmad, P., 2020. Influence of exogenous salicylic acid and nitric oxide on growth, photosynthesis, and ascorbate-glutathione cycle in salt stressed *Vigna angularis*. Biomolecules 10, 42. https://doi.org/10.3390/biom10010042.

Allel, D., Ben-Amar, A., Abdelly, C., 2018. Leaf Photosynthesis, chlorophyll fluorescence and ion content of barley (*Hordeum vulgare*) in response to salinity. J. Plant Nutr. 41, 497–508. https://doi.org/10.1080/01904167.2017.1385811.

Alvarez-Pizarro, J.C., Gomes-Filho, E., Prisco, J.T., Grossi-de-Sá, M.F., Oliveira-Neto, O. B., 2011. NH_4^+ -stimulated low-K^+ uptake is associated with the induction of H^+ extrusion by the plasma membrane H^+- ATPase in sorghum roots under K^+ deficiency. J. Plant Physiol. 168, 1617–1626. https://doi.org/10.1016/j.jplph.2011.03.002.

Araújo, G.S., Paula-Marinho, S.O., Pinheiro, S.K.P., Miguel, E.C., Lopes, L.S., et al., 2021. H_2O_2 priming promotes salt tolerance in maize by protecting chloroplasts ultrastructure and primary metabolites modulation. Plant Sci. 303, 110774. https://doi.org/10.1016/j.plantsci.2020.110774.

Baena, G., Feria, A.B., Echevarría, C., Monreal, J.A., García-Mauriño, S., 2017. Salinity promotes opposite patterns of carbonylation and nitrosylation of C_4 phosphoenolpyruvate carboxylase in sorghum leaves. Planta 246, 1203–1214. https://doi.org/10.1007/s00425-017-2764-y.

Basu, S., Duren, W., Evans, C.R., Burant, C.F., Michailidis, G., Karnovsky, A., 2017. Systems biology sparse network modeling and metscape-based visualization methods for the analysis of large-scale metabolomics data. Bioinformatics 33, 1545–1553. https://doi.org/10.1093/bioinformatics/btx012.

Beers, Jr. R.F., Sizer, I.W., 1952. A spectrophotometric method for measuring the breakdown of hydrogen peroxide by catalase. J. Biol. Chem. 195, 133–140.

Beyer, W.F., Fridovich, I., 1987. Assaying for superoxide dismutase activity: some large consequences of minor changes in conditions. Anal. Biochem. 161, 559–566. https://doi.org/10.1016/0003-2697(87)90489-1.

Boschiero, B.N., Mariano, E., Azevedo, R.A., Trivelin, P.C.O., 2019. Influence of nitrate-ammonium ratio on the growth, nutrition, and metabolism of sugarcane. Plant Physiol. Biochem. 139, 246–255. https://doi.org/10.1016/j.plaphy.2019.03.024.

Bradford, M.M., 1976. A rapid and sensitive method for the quantification of microgram quantities of protein utilizing the principle of protein-dye binding. Anal. Biochem. 72, 246–254. https://doi.org/10.1016/0003-2697(76)90527-3.

Cardoso, L.L., Freire, F.B.S., Daloso, D.M., 2023. Plant metabolic networks under stress: a multi-species/stress condition meta-analysis. J. Soil Sci. Plant Nutr. 23, 4–21. https://doi.org/10.1007/s42729-022-01032-2.

Chang, J., Cheong, B.E., Natera, S., Roessner, U., 2019. Morphological and metabolic responses to salt stress of rice (*Oryza sativa* L.) cultivars which differ in salinity tolerance. Plant Physiol. Biochem. 144, 427–435. https://doi.org/10.1016/j.plaphy.2019.10.017.

Coelho, D.G., Miranda, R.S., Paula-Marinho, S.O., Carvalho, H.H., Prisco, J.T., Gomes-Filho, E., 2020. Ammonium nutrition modulates K^+ and N uptake, transport and accumulation during salt stress acclimation of sorghum plants. Arch. Agron Soil Sci. 66, 1991–2004. https://doi.org/10.1080/03650340.2019.1704736.

de Souza, E.A.C.C., Alvarez-Pizarro, J.C., Lopes, L.S., Miranda, R.S., Gomes-Filho, E., 2021. Nitrate and ammonium nutrition modulates the photosynthetic performance and antioxidant defense in salt-stressed grass species. J. Soil Sci. Plant Nutr. 21, 3016–3029. https://doi.org/10.1007/s42729-021-00586-x.

Echevarria, C., Pacquit, V., Bakrim, N., Osuna, L., Delgado, B., Arriodupont, M., Vidal, J., 1994. The effect of pH on the covalent and metabolic control of C4 phosphoenolpyruvate carboxylase from Sorghum leaf. Arch. Biochem. Biophys. 315, 425–430. https://doi.org/10.1006/abbi.1994.1520.

Elstner, E.F., Heupel, A., 1976. Inhibition of nitrite formation from hydroxyl ammonium chloride: a simple assay for superoxide dismutase. Anal. Biochem. 70, 616–620. https://doi.org/10.1016/0003-2697(76)90488-7.

Fernández-Crespo, E., Gómez-Pastor, R., Scalschi, L., Llorens, E., Camañes, G., García-Agustín, P., 2014. NH_4^+ induces antioxidant cellular machinery and provides resistance to salt stress in citrus plants. Trees (Berl.) 28, 1693–1704. https://doi.org/10.1007/s00468-014-1078-y.

Fernando, C.D., Soysa, P., 2015. Optimized enzymatic colorimetric assay for determination of hydrogen peroxide (H_2O_2) scavenging activity of plant extracts. MethodsX 2, 283–291. https://doi.org/10.1016/j.mex.2015.05.001.

Freitas, V.S., Miranda, R.S., Costa, J.H., Oliveira, D.F., Paula, S.O., et al., 2018. Ethylene triggers salt tolerance in maize genotypes by modulating polyamine catabolism enzymes associated with H_2O_2 production. Environ. Exp. Bot. 145, 75–86. https://doi.org/10.1016/j.envexpbot.2017.10.022.

González-Hernández, A.I., Fernández-Crespo, E., Scalschi, L., Hajirezaei, M., Wirén, N.V., et al., 2019. Ammonium mediated changes in carbon and nitrogen metabolisms induce resistance against *Pseudomonas syringae* in tomato plants. J. Plant Physiol. 239, 28–37. https://doi.org/10.1016/j.jplph.2019.05.009.

Guidi, L., Lo Piccolo, E., Landi, M., 2019. Chlorophyll fluorescence, photoinhibition and abiotic stress: does it make any difference the fact to Be a C3 or C4 species? Front. Plant Sci. 10, 174. https://doi.org/10.3389/fpls.2019.00174.

Heath, R.L., Packer, L., 1968. Photoperoxidation in isolated chloroplasts: I. Kinetics and stochiometry of fatty acid peroxidation. Arch. Biochem. Biophys. 125, 189–198. https://doi.org/10.1016/0003-9861(68)90654-1.

Hessini, K., Issaoui, K., Ferchichi, S., Saif, T., Abdelly, C., Siddique, K.H.M., Cruz, C., 2019. Interactive effects of salinity and nitrogen forms on plant growth, photosynthesis and osmotic adjustment in maize. Plant Physiol. Biochem. 139, 171–178. https://doi.org/10.1016/j.plaphy.2019.03.005.

Huang, H., Ullah, F., Zhou, D.-X., Yi, M., Xhao, Y., 2019. Mechanisms of ROS regulation of plant development and stress responses. Front. Plant Sci. 10, 800. https://doi.org/10.3389/fpls.2019.00800.

Hualpa-Ramirez, E., Carrasco-Lozano, E.C., Madrid-Espinoza, J., Tejos, R., Ruiz-Lara, S., Stange, C., Norambuena, L., 2024. Stress salinity in plants: new strategies to cope with in the foreseeable scenario. Plant Physiol. Biochem. 208, 108507. https://doi.org/10.1016/j.plaphy.2024.108507.

Ivanov, B.N., 2014. Role of ascorbic acid in photosynthesis. Biochemistry 79, 282–289. https://doi.org/10.1134/S0006297914030146.

Jia, X.-M., Zhu, Y.-F., Hu, Y., Zhang, R., Cheng, L., Zhu, Z.-L., Zhao, T., Zhang, X., Wang, Y.-X., 2019. Integrated physiologic, proteomic, and metabolomic analyses of *Malus halliana* adaptation to saline-alkali stress. Hortic. Res. 6, 91. https://doi.org/10.1038/s41438-019-0172-0.

Kronzucker, H.J., Coskun, D., Schulze, L.M., Wong, J.R., Britto, D.T., 2013. Sodium as nutrient and toxicant. Plant Soil 369, 1–23. https://doi.org/10.1007/s11104-013-1801-2.

Lacerda, C.F., Cambraia, J., Oliva, M.A., Ruiz, H.A., 2005. Changes in growth and in solute concentrations in sorghum leaves and roots during salt stress recovery. Environ. Exp. Bot. 54, 69–76. https://doi.org/10.1016/j.envexpbot.2004.06.004.

Li, Z.-G., 2024. Ammonia: an emerging gasotransmitter in plant growth and response to environmental stress. J. Plant Growth Regul. 43, 3958–3970. https://doi.org/10.1007/s00344-024-11391-y.

Liang, Y., Liu, H., Fu, Y., Li, P., Li, S., Gao, Y., 2023. Regulatory effects of silicon nanoparticles on the growth and photosynthesis of cotton seedlings under salt and low-temperature dual stress. BMC Plant Biol. 23, 504. https://doi.org/10.1186/s12870-023-04509-z.

Lisec, J., Schauer, N., Kopka, J., Willmitzer, L., Fernie, A.R., 2006. Gas chromatography mass spectrometry-based metabolite profiling in plants. Nat. Protoc. 1, 387–396. https://doi.org/10.1038/nprot.2006.59.

Malavolta, E., Vitti, G.C., Oliveira, S.A., 1989. Avaliação do estado nutricional das plantas; princípios e aplicações, Ed. 1, pp. 1–201. Piracicaba: Potafos.

Manaa, A., Goussi, R., Derbali, W., Cantamessa, S., Abdelly, C., Barbato, R., 2019. Salinity tolerance of quinoa (*Chenopodium quinoa* Willd) as assessed by chloroplast ultrastructure and photosynthetic performance. Environ. Exp. Bot. 162, 103–114. https://doi.org/10.1016/j.envexpbot.2019.02.012.

Marco, P., Carvajal, M., Martínez-Ballesta, M.D.C., 2019. Efficient leaf solute partitioning in *Salicornia fruticose* allows growth under salinity. Environ. Exp. Bot. 157, 177–186. https://doi.org/10.1016/j.envexpbot.2018.10.001.

Miranda, R.S., Alvarez-Pizarro, J.C., Araújo, C.M.S., Prisco, J.T., Gomes-Filho, E., 2013. Influence of inorganic nitrogen sources on K^+/Na^+ homeostasis and salt tolerance in sorghum plants. Acta Physiol. Plant. 35, 841–852. https://doi.org/10.1007/s11738-012-1128-2.

Miranda, R.S., Gomes-Filho, E., Prisco, J.T., Alvarez-Pizarro, J.C., 2016. Ammonium improves tolerance to salinity stress in *Sorghum bicolor* plants. Plant Growth Regul. 78, 121–131. https://doi.org/10.1007/s10725-015-0079-1.

Miranda, R.S., Mesquita, R.O., Costa, J.H., Alvarez-Pizarro, J.C., Prisco, J.T., Gomes-Filho, E., 2017. Integrative control between proton pumps and SOS1 antiporters in roots is crucial for maintaining low Na^+ accumulation and salt tolerance in ammonium-supplied *Sorghum bicolor*. Plant Cell Physiol. 58, 522–536. https://doi.org/10.1093/pcp/pcw231.

Mittler, R., 2017. ROS are good. Trends Plant Sci. 22, 11–19. https://doi.org/10.1016/j.tplants.2016.08.002.

Munns, R., Day, D.A., Fricke, W., Watt, M., Arsova, B., Barkla, B.J., Bose, J., Byrt, C.S., Chen, Z.-H., Foster, K.J., Gilliham, M., Henderson, S.W., Jenkins, C.L.D., Kronzucker, H.J., Miklavcic, S.J., Plett, D., Roy, S.J., Shabala, S., Shelden, M.C., Soole, K.L., Taylor, N.L., Tester, M., Wege, S., Wegner, L.H., Tyerman, S.D., 2020. Energy costs of salt tolerance in crop plants. New Phytol. 225, 1072–1090. https://doi.org/10.1111/nph.15864.

Nakano, Y., Asada, K., 1981. Hydrogen peroxide is scavenged by ascorbate-specific peroxidase in spinach chloroplasts. Plant Cell Physiol. 22, 867–880. https://doi.org/10.1093/oxfordjournals.pcp.a076232.

Oliveira, F.D.B., Miranda, R.S., Araújo, G.D.S., Coelho, D.G., Lobo, M.D.P., Paula-Marinho, S.O., Lopes, L.S., Monteiro-Moreira, A.C.O., Carvalho, H.H., Gomes-Filho, E., 2020. New insights into molecular targets of salt tolerance in sorghum leaves elicited by ammonium nutrition. Plant Physiol. Biochem. 154, 723–734. https://doi.org/10.1016/j.plaphy.2020.06.051.

Omoto, E., Nagao, H., Taniguchi, M., Miyake, H., 2013. Localization of reactive oxygen species and change of antioxidant capacities in mesophyll and bundle sheath chloroplasts of maize under salinity. Physiol. Plantarum 149, 1–12. https://doi.org/10.1111/ppl.12017.

Ortiz-Espín, A., Sánchez-Guerrero, A., Sevilla, F., Jiménez, A., 2018. The role of ascorbate in plant growth and development. In: Hossain, M.A., Munné-Bosch, S., Burritt, D., Diaz-Vivancos, P., Fujita, M., Lorence, A. (Eds.), Ascorbic Acid in Plant Growth, Development and Stress Tolerance. Springer, Cham, pp. 25–45. https://doi.org/10.1007/978-3-319-74057-7_2.

Panda, A., Rangani, J., Parida, A.K., 2021. Unraveling salt responsive metabolites and metabolic pathways using non-targeted metabolomics approach and elucidation of salt tolerance mechanisms in the xero-halophyte *Haloxylon salicornicum*. Plant Physiol. Biochem. 158, 284–296. https://doi.org/10.1016/j.plaphy.2020.11.012.

Rajkumari, N., Chowrasia, S., Nishad, J., Ganie, S.A., Mondal, T.K., 2023. Metabolomics-mediated elucidation of rice responses to salt stress. Planta 258, 111. https://doi.org/10.1007/s00425-023-04258-1.

Seo, S.Y., Kim, Y.J., Park, K.Y., 2019. Increasing polyamine contents enhances the stress tolerance via reinforcement of antioxidative properties. Front. Plant Sci. 10, 1331. https://doi.org/10.3389/fpls.2019.01331.

Singh, M., Singh, V.P., Prasad, S.M., 2019. Nitrogen alleviates salinity toxicity in *Solanum lycopersicum* seedlings by regulating ROS homeostasis. Plant Physiol. Biochem. 141, 466–476. https://doi.org/10.1016/j.plaphy.2019.04.004.

Souza, G.M., Lüttge, U., 2015. Stability as a phenomenon emergent from plasticity–complexity–diversity in eco-physiology. In: Lüttge, U., Beyschlag, W. (Eds.), Progress in Botany, vol. 76. Springer, Cham, pp. 211–239. https://doi.org/10.1007/978-3-319-08807-5_9.

Sweetlove, L.J., Fernie, A.R., 2005. Regulation of metabolic networks: understanding metabolic complexity in the systems biology era. New Phytol. 168, 9–24. https://doi.org/10.1111/j.1469-8137.2005.01513.x.

Taïbi, K., Taïbi, F., Ait Abderrahim, L., Ennajah, A., Belkhodja, M., Mulet, J.M., 2016. Effect of salt stress on growth, chlorophyll content, lipid peroxidation and antioxidant defence systems in *Phaseolus vulgaris* L. South Afr. J. Bot. 105, 306–312. https://doi.org/10.1016/j.sajb.2016.03.011.

Tavakoli, R., Hajiboland, R., Haeili, M., Sadeghzadeh, N., Nikolic, M., 2025. Effect of elevated ammonium on biotic and abiotic stress defense responses and expression of related genes in cucumber (*Cucumis sativus* L.) plants. Plant Physiol. Biochem. 218, 109310. https://doi.org/10.1016/j.plaphy.2024.109310.

Urbanek, H., Kuzniak-Gebarowska, E., Herka, K., 1991. Elicitation of defense responses in bean leaves by *Botrytis cinereal* polygalacturonase. Acta Physiol. Plant. 13, 43–50.

Wungrampha, S., Joshi, R., Singla-Pareek, S.L., Pareek, A., 2018. Photosynthesis and salinity: are these mutually exclusive? Photosynthetica 56, 366–381. https://doi.org/10.1007/s11099-017-0763-7.

Zayed, O., Hewedy, O.A., Abdelmoteleb, A., Ali, M., Youssef, M.S., Roumia, A.F., Seymour, D., Yuan, Z.-C., 2023. Nitrogen journey in plants: from uptake to metabolism, stress response, and microbe interaction. Biomolecules 13, 1443. https://doi.org/10.3390/biom13101443.

Zhou, Y., Feng, C., Wang, Y., Yun, C., Zou, X., Chen, N., Zhang, W., Jing, Y., Li, H., 2024. Understanding of plant salt tolerance mechanisms and application to molecular breeding. Int. J. Mol. Sci. 25, 10940. https://doi.org/10.3390/ijms252010940.

Zhu, C.Q., Zhang, J.H., Zhu, L.F., Abliz, B., Zhong, C., Bai, Z.G., Hu, W.J., Sajid, H., James, A.B., Cao, X.C., Jin, Q.Y., 2018. NH_4^+ facilitates iron reutilization in the cell walls of rice (*Oryza sativa*) roots under iron-deficiency conditions. Environ. Exp. Bot. 151, 21–31. https://doi.org/10.1016/j.envexpbot.2018.03.018.

Zi, Y., Zhu, L., Ma, Y., Hong, L., Wang, S., Zhao, G., 2024. Integrative analysis of transcriptome and metabolome provides insights into the saline-alkali stress in alfalfa. Russ. J. Plant Physiol. 71, 219. https://doi.org/10.1134/S1021443724607390.